Journal of Vibration Engineering & Technologies (2023) 11:1889–1901
https://doi.org/10.1007/s42417-022-00677-8

ORIGINAL PAPER

Numerical Investigation of Eigenvalue Characteristics (Vibration and Buckling) of Damaged Porous Bidirectional FG Panels

Priyanshu Hissaria[1] · Prashik Malhari Ramteke[1] · Chetan Kumar Hirwani[2] · S. R. Mahmoud[3] · Erukala Kalyan Kumar[1] · Subrata Kumar Panda[1]

Received: 12 July 2022 / Revised: 11 August 2022 / Accepted: 14 August 2022 / Published online: 1 September 2022

Abstract

Purpose The present research work aims to analyze the vibration and buckling behaviour of multidirectional FG porous structures engrained with damage. Power-law (P-FGM), sigmoid (S-FGM) and exponential (E-FGM) gradings are considered to compute the material properties of the cracked FG plate. The porosity effect on the structural strength has been modelled to explore the realistic influences.

Methods In the current study, the eigenvalue analysis of the cracked FG plate with porosities is performed computationally with the help of a numerical model. The multidirectional porous structural model is repaired in ABAQUS via python script to meet the batch input. The study used the ABAQUS kernel instead of the standard GUI for better control.

Results The adequacy of the current model has been verified initially by comparing the eigenvalues (frequency and buckling load) with those of available published data with and without damages (crack). The results have been calculated for different grading patterns, porosity values, geometrical data, grading index, and crack-dependent parameters to understand their influence on the eigenvalues of the damaged multidirectional porous graded structures.

Conclusions A few generalized understandings are obtained based on the parametric study, i.e., the cracks cause a substantial decrement in total structural stiffness, which, in turn, reduces the final results adequately. Structural components are affected due to the presence of a crack in specific orientations, like in the lengthier edge of the rectangular shape. Similarly, the porosity affects the total stiffness and associated responses like the frequency and the critical buckling load.

Keywords Functionally graded materials · Vibration and buckling analysis · Bidirectional grading · Crack · Porosity

✉ Subrata Kumar Panda
pandaskmosclass@gmail.com; pandask@nitrkl.ac.in

Priyanshu Hissaria
md.priyanshu@gmail.com

Prashik Malhari Ramteke
prashikramteke793@gmail.com

Chetan Kumar Hirwani
chetank.me@nitp.ac.in

S. R. Mahmoud
Samsam73@yahoo.com

Erukala Kalyan Kumar
kalyan.me320@gmail.com

[1] Department of Mechanical Engineering, National Institute of Technology Rourkela, Rourkela, Odisha 769008, India

[2] Department of Mechanical Engineering, National Institute of Technology Patna, Patna, Bihar 800005, India

[3] GRC Department, Applied College, King Abdulaziz University, Jeddah 21589, Saudi Arabia

Abbreviations

ANN	Artificial neural networks
SSSS	All sides simply supported
E-FGM	Exponential FGM
XIGA	Extended isogeometric analysis
XFEM	Extended finite element method
FGM	Functionally graded materials
GUI	Graphic user interface
PFGM	Porous FGM
P-FGM	Power-law FGM
S-FGM	Sigmoid FGM
UDL	Uniformly distributed load

List of Symbols

d	Crack length
a, b and h	Length, width, and thickness of the FG plate
$G(z, x)$	Material property of FGM
ρ	Mass density
ρ_m and ρ_c	Mass density of metal and ceramic
ω	Natural frequency

ν	Poison's ratio
ν_m and ν_c	Poison's ratio for metal and ceramic
λ	Porosity index
n_x and n_z	Power-exponents in x and z-directions
G_1, G_2	Properties of metal and ceramic
λ_{cru} and λ_{crb}	Unidirectional and bidirectional critical buckling load
V_f	Volume fraction of ceramic
E_m and E_c	Young's modulus of metal and ceramic material

Introduction

Functionally graded materials (FGM) are considered as special race of composites but different from normal ones, where layers with different properties are combined to form a single structure. The main difference is that due to the techniques used in developing FGMs, the material properties vary following a particular function. The layers are combined on a microscopic level, making it seem like new material. For a long time, it was believed that functionally graded materials are prone to cracks and delamination, unlike normal composite materials, due to their microscopically distributed properties. Still, in recent years, it has been observed that these materials can also develop cracks type defects in severe environments. Therefore, a deep study of cracked FGM structures under different loading conditions becomes essential. In this study, the authors are going to find the variation in natural frequency of a simply supported cracked bidirectional FGM plate with a variation in different parameters such as plate geometry, crack length, porous nature of the material, as well as the variation profile of the material using different functional laws. Also, the buckling behavior of a simply supported cracked bidirectional FGM plate with different parameters such as crack length, plate geometry, material variation profile, and porosity value is studied in the present article since buckling can occur quite a lot in thin plates, such a mode of crisis can often causes the failure of strength. Both studies are performed using ABAQUS software for finite element analysis, in which the plate with multiple layers having different properties is constructed using a python script. As the plate is bidirectionally graded, the material properties vary along the x and z-directions with grading index n_x and n_z.

FGM has been a hot topic of study in the past few years due to their wide variety of use in places where normal materials cannot hold their own. A study in [1] presented the solution for vibration along with buckling problems for a simple plate cracked from one edge and a plate which would have an crack located internally in the center of the plate. These problems were formulated as dual series equations and diminished to second-type homogenous Fredholm integral equations. Buckling loads for cracked plates at the edge or the center are estimated [2] using hierarchical trigonometric functions to outline the displacement function of the damaged plate. They used a Discrete Kirchoff-Mindlin Triangular element in the analysis of the plate with cracks of different sizes. Buckling response of various cracked elastic plates exposed to tension or compressive load while taking care of the effects of mechanical, geometrical, as well as different boundary conditions, and varying crack lengths and orientations are analyzed [3]. In this case, the nonlinear analysis was performed with crack faces interaction taken into account. Buckling analysis of curvilinearly laminated composite plates for arbitrarily shaped cutouts is examined utilizing isogeometric analysis [4, 5], and the same analysis is performed to periodically supported beams and verified using ABAQUS simulation software [6]. Thermal post-buckling properties of porous composite nanoplates made of an FGM with a central cutout of various shapes are investigated [7] utilizing a surface elastic-based 3D nonlinear formulation. The buckling analysis of homogeneous, isotropic, regular hexagonal thin sheets under in-plane hydrostatic and uniaxial compression is investigated in [8].

Some researchers [9, 10] used the Bernoulli–Euler beam theory, as well as the rotational spring model, to investigate frequency responses as well as elastic buckling of functionally graded materials for different types of boundary conditions, number, and locations of cracks, etc. Similarly, a few studies [11, 12] investigated the buckling behvaiour of the unidirectional FGM plate exposed to thermo-mechanical load using an improved higher-order shear deformation plate theory to compensate for the transverse shear strains by keeping top and bottom faces stress-free. Reddy's third-order plate theory was used in [13] along with a novel Ritz procedure including additional functions on a unidirectional FGM plate according to P-FGM to find the effect of parameters such as slenderness ratio, power-law coefficient, etc. on the natural frequency of side crack containing FGM plate. Using the extended Q4 formulation [14] showed the FEA of functionally graded crack containing plate to find the natural frequencies. Classic plate theory was used by [15] through the FE approach to find the critical buckling load of cracked FGM plate under uniaxial and biaxial tension and varying parameters such as grading index. Combining the extended isogeometric method, as well as HSDT [16], natural frequencies at different modes of cracked FGM plates of different geometries and the properties varying in the thickness direction according to E-FGM type were found out. The functionally graded structure's vibration and thermal buckling responses were reported in [17] using FEA and first-order theory. The developments of vibrational studies of small structures utilizing nonlocal/nonclassical continuum theories are reviewed, mainly emphasizing small beam-like structures [18]. The nonlinear large-amplitude natural

frequency responses of nanoshells made of porous FGM by taking vibrational mode interactions and surface stress size effects into account are analyzed [19]. A light sandwich plate's damped vibrational behavior under periodic load for a finite amount of of time is investigated [20]. To estimate the minor effects on the nonlinear instability characteristics of hydrostatic pressurized FGM microsized shells, a nonlocal strain gradient shell model is applied [21]. A detailed review is carried on natural frequency analysis of small-scaled plate-based structures [22]. Lazreg Hadji et al. focused on the eigenvalue responses of an imperfect FG sandwich plate [23] and FG Porous Sandwich Plates [24], which consists of an isotropic homogeneous core that rests on an elastic foundation and porous face sheets made of FGMs. Natural frequencies of imperfect S-FGM and P-FGM beams [25] and porous FG nanobeams using hyperbolic shear deformation beam theory [26] are investigated.

An 8-noded degenerated shell element was used for the extended FEA [27] for buckling analysis of crack containing composite plates, also involving transverse shear deformation effects. Rectangular and circular cracked composite plates were analyzed with varying crack sizes and locations, as well as a number of cracks. Using the extended FE method, [28] incorporated the discrete shear gap method to remove the shear locking on an accurately extended 3-node triangular plate element to study the buckling type failure analysis of crack containing FGM plates exposed to either uniaxial or biaxial compression loads. Singular convolution approach was used [29] in to discretize the differential equation for buckling of the laminated panel. Another study [30] presented the XFEM formulation of vibrational behavior of five different FGM shell models of different geometry with cracks present in them and the effects of different parameters on the natural frequencies of these models. Using Berger's formulation to include nonlinearity, as well as Galerkin's method to solve governing differential equation, [31] presented a nonlinear analytical model to show the effect of crack orientation, size, as well as aspect ratio in the vibrational analysis of FGM plates containing a crack. Based on FSDT and Von-Karman's theory, [32, 33] used an extended Ritz formulation on multilayered composite cracked plates for buckling and post-buckling analysis.

Extended isogeometric analysis (XIGA) [34] was used through the cracked plate, with the help of Reddy's HSDT using a Ritz approach, [35] presented the buckle and post-buckling analysis of simple cracked plates. In a study, [36] the transient response of a unidirectional porous FGM plate with patterns was presented and the different types of functions generally used in FGM technology were explained. Bifurcation buckling of the FGM plate has been presented [37, 38], and critical buckling loads have been found for all the different boundary conditions for which bifurcation buckling is possible. In another study [39], the vibration and cracked identification of P-FGM plates with through width edge cracks were presented. The crack was modeled as a massless rotational spring, and the SIF was calculated using the Mindlin plate theory and differential quadrature method to determine the spring stiffness. Artificial neural network method was used [40] to predict natural frequencies of simple supported P-FGM plates of different materials, crack lengths, porosity values, crack orientation and power-law index using Navier's solution after using Hamilton's principle to derive equations of motion. Another study [41]- presented the vibrational response of multidirectional FGM plate using different grading functions, as well as even or uneven porosity values. The material variation in multidirectional grading is explained with the equations of all three laws, also, in [42], the transient response of multidirectional FGM plate using ANSYS, MATLAB and Python code in ABAQUS are computed.

Using the asymptotic numerical method and thin plate kinematics of von Karman, [43] proposed buckling and post-buckling analysis of an FGM plate. In one study [44], a side cracked thin rectangular plate was separated into sub-plates, which were then put into the Hamiltonian system and analytically solved using the symplectic superposition approach. Another study [45] proposed quantification and localization approaches to detect the damage in FGM plates employing Frequency Response Function and ANN, as well as Arithmetic Optimization Algorithm for damage quantification. Some researchers [46, 47] investigated the natural frequency and critical buckling load of multidirectional porous FGM sandwich plates where material properties varied based on Voigt's micro-mechanical model according to P-FGM distribution. One study [48] reviewed the effect of the formation of a crack on the eigen frequency responses of the FGM component.

It is observed from the review of the articles that a lot of research in the field of vibration and buckling is available on FG structure. The majority of the research focused on the structural analysis of unidirectional FGM with a P-FGM type of grading pattern without damage. Moreover, none of the analyses performed to study the frequency and buckling characteristics of bidirectional FG panels associated with the crack and porosity type of defects. Hence, to address the same, the goal of the present research is to develop a generalized computational facility for the eigenvalue (vibration and buckling) of the graded structure with and without crack and porosity type of defects. Also, the present model utilizes all three kinds of grading patterns (P-FGM, S-FGM and E-FGM). The accuracy of the developed model is verified using a validation test. Using a validation test, the created model's accuracy is checked. The next step is to conduct the parametric analysis to delibirate the influence of various design factors on the eigenvalue charactaristics of the bidirectional FG panel.

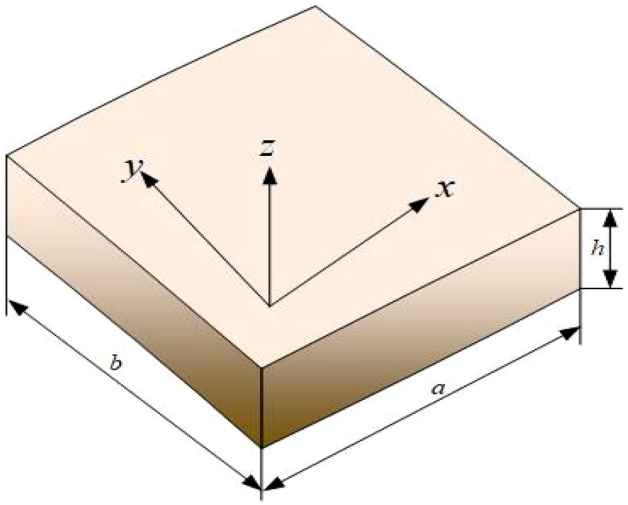

Fig. 1 The geometry of bidirectional FG plate

Methodology

The geometry of the bidirectional FG plate is shown in Fig. 1. The grading along thickness and length direction is shown in Fig. 2. Figure 3 displays the crack geometry, and Fig. 4 shows the porosity distribution inside the FG plate. Here a and b denote the length and width of the FG plate, respectively. h denotes the thickness of FG plate. Crack length is denoted by d. The material variation in the FG plate follows various grading patterns as discussed in the below subsection.

Material Properties of the Graded Panel

Variation of material properties in the FG structure follows a particular function in a specific direction. Three different forms of material grading patterns are used in the current work considering uni/bidirectional material property variation.

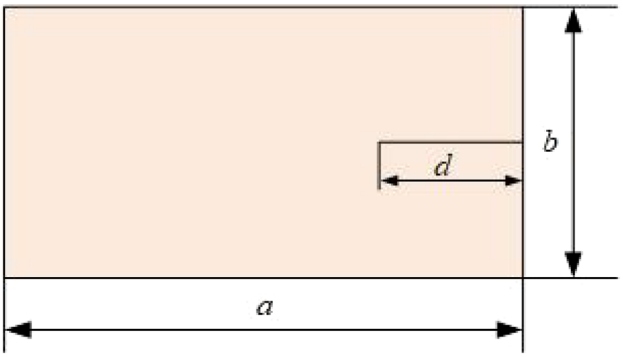

Fig. 3 Crack geometry

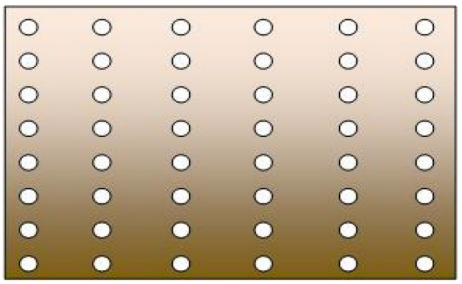

Fig. 4 Porosity distribution inside the FG plate

E-FGM

The properties change according to the mathematical exponential function in this material variation profile. The mathematical formulation for the same can be given in terms of material one and material two with varying volume fractions. The mathematical formula for any property, $G(z, x)$, considering bidirectional grading [49], is as follows:

$$G(z,x) = G_1 e^{\left(\frac{-1}{2}\ln\left(\frac{G_1}{G_2}\right)\left(1-\frac{2z}{h}\right)\left(\frac{x}{a}\right)^{n_x}\right)} \quad (1)$$

Similarly, for bidirectional grading with even porosity (having porosity index λ):

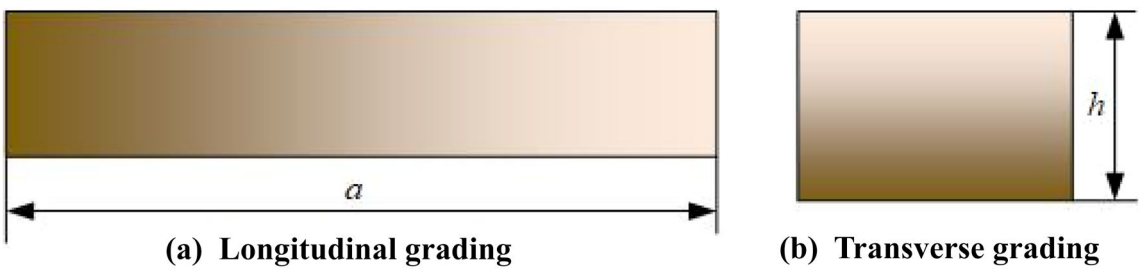

Fig. 2 **a** The grading along the thickness direction, **b** The grading along the length direction

$$G(z,x) = G_1 e^{\left(\frac{-1}{2}\ln\left(\frac{G_1}{G_2}\right)\left(1-\frac{2z}{h}\right)\left(\frac{x}{a}\right)^{n_x} - 0.5\lambda\ln\left(\frac{G_1}{G_2}\right)\right)} \quad (2)$$

where, G_1 and G_2 are the properties of metal and ceramic, respectively. n_x is the material variation profiles in the x-direction.

P-FGM

The exponential function provides only one pattern for specific materials combination, but P-FGM provides a number of grading patterns. This grading method uses the volume fraction index to define the property of a layer. The volume fraction has a material variation profile factor. This factor is also known as the volume fraction exponent, or simply, the power-law coefficients. The mathematical formulation [50] of any property, $G(z, x)$, at any location is given by:

$$G(z,x) = (G_1 - G_2)V_f + G_2 \quad (3)$$

Here the volume fraction (V_f) is defined for P-FGM as follows:

$$V_f = \left(\frac{1}{2} + \frac{z}{h}\right)^{n_z}\left(\frac{x}{a}\right)^{n_x} \quad (4)$$

where, n_z is the volume fraction exponents in the thickness direction.

The expression of $G(z, x)$ for bidirectional grading with even porosity [51] is given by:

$$G(z,x) = (G_1 - G_2)V_f + G_2 - 0.5\lambda(G_1 + G_2) \quad (5)$$

S-FGM

When a single power-law function FGM is added to multilayered composite structures, the stress concentrations happen at a particular interface where the structure's material variation is smooth yet changes quickly.

Due to this problem, Chung and Chi in 2006 [50] formulated a new volume fraction using two power-law functions, as expressed in Eq. (6). It is done to make the stress distribution smooth all over the structure.

$$V_f = \begin{cases} \left[1 - 0.5\left(1 - \frac{2z}{h}\right)^{n_z}\left(\frac{x}{a}\right)^{n_x}\right] \; for \; 0 \le z \le \frac{h}{2} \\ \left[0.5\left(1 + \frac{2z}{h}\right)^{n_z}\left(\frac{x}{a}\right)^{n_x}\right] \; for \; -\frac{h}{2} \le z \le 0 \end{cases} \quad (6)$$

For unidirectional grading, the value of n_x will become zero, i.e. the power-law exponent in the length direction will become null.

Methodology

A simulation tool, ABAQUS, provided by Dassault System, is used to perform the FEA of the FGM plate with or without crack and porosity. In ABAQUS, specific steps are required to follow to complete the analysis, which are described below:

- A 3D planar shell-type element was created in the 'create part' section, forming a square plate.
- Selecting the 'create partition' option, partitions along the x-axis are created equal to the number of layers.
- Created the required number of materials with calculated properties using the materials section.
- Selecting each partition created, composite layups equal to the number of layers along the x-axis were created with number of plys equal to the number of layers along the z-axis. In this way, a number of layers (side layers × down layers) are created in total, each having its properties according to the function.
- In the Interaction section, a particular option was selected from the menu bar. Then, the crack → assign seam option was selected, and the crack region was chosen for assigning the seam.
- In the assembly section, create new instance option was selected, and assembly was created.
- Based on the type of analysis, steps were created in the create step section.
- SSSS boundary conditions were given to the plate in the load section, and the mechanical load was applied.
- The mesh section defined mesh geometry and setting, and meshing was created according to the required mesh size.
- In the job section, a new job was created and then submitted.
- In the visualization section, the deformed plate was visible. By selecting the results option in the menu bar, eigenvalues for different modes can be found, and the plate orientation on each mode can be seen.

A flow chart procedure for the static and transient deflection analysis of the FG plate is presented in Fig. 5. The layers of the bidirectional FG plate along the length and transverse direction can be seen in Fig. 6 and Fig. 7, respectively.

Automation

The following steps are followed to make the script for the analysis of the FG plate:

- Using the macro manager option available in ABAQUS, a work macro created and started making the model. Macro for a simple plate, having a small number of layers and SSSS boundary conditions was developed.

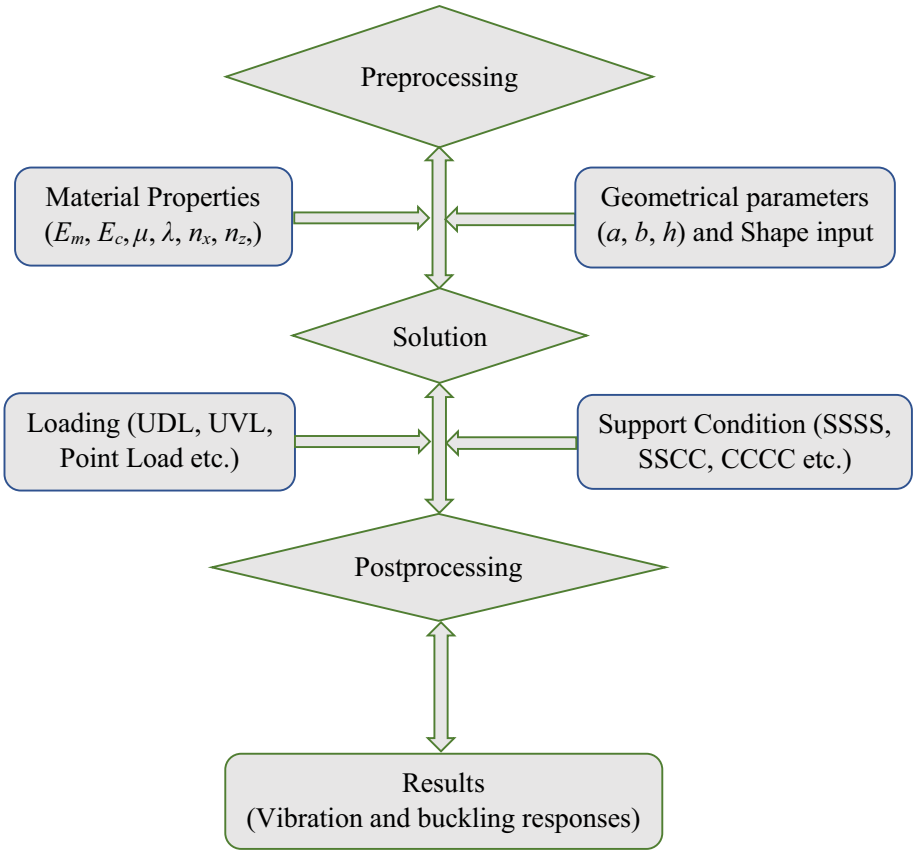

Fig. 5 Simulation procedure for eigenvalue analysis of FG plate

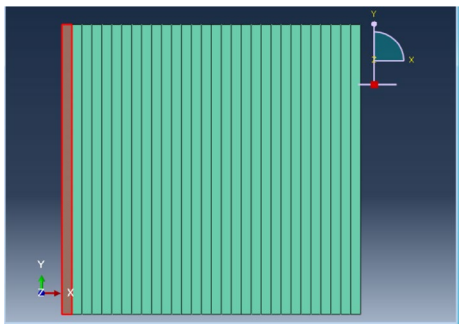

Fig. 6 Bidirectional graded FGM layers along the x-axis in ABAQUS

- The composite layup feature was used to provide different properties to each layer.
- The functions are utilized (Eqs. 1–6) to create materials according to the required grading pattern. The materials are assigned to each layer with their location only.
- Different scripts were created for different analysis types, such as vibration and buckling analysis, with and without crack. Also, the unidirectional and multidirectional grading formulas were incorporated into other scripts.
- After the FGM plate was created and analyzed, a simple plate was made, and then a crack was generated in the plate. The coding part for crack generation was recorded using the macro manager.
- The program for generating cracks in a simple plate was incorporated into different analysis scripts of simple FGM plates.
- Using the Python scripts, results were computed and validated for the natural frequency and buckling analysis of the cracked multidirectional FGM plate. The new results are then generated for the different parameters.

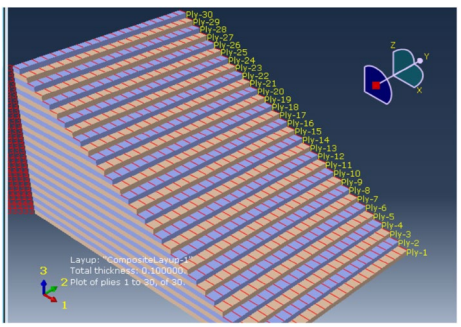

Fig. 7 Layers along the z-axis in Bidirectional graded plates in ABAQUS

Table 1 The first three non-dimensional natural frequencies of a SSSS square FG plate with a horizontal side crack ($a/b=1$, $h/a=0.1$, $d=0.5a$)

Gradient index	Mode 1			Mode 2			Mode 3		
	Ref. [14]	Present	% diff	Ref. [14]	Present	% diff	Ref. [14]	Present	% diff
0	5.387	5.437	0.933	11.419	11.769	3.068	13.359	13.521	1.216
0.2	5.028	5.023	0.102	10.659	10.922	2.463	12.437	12.555	0.949
1	4.122	4.158	0.865	8.526	9.087	6.574	10.285	10.374	0.865
5	3.626	3.552	2.033	7.415	7.569	2.081	8.566	8.749	2.132
10	3.409	3.440	0.898	7.059	7.273	3.039	8.221	8.443	2.706

Results and Discussion

After successfully making the FEA model of cracked bidirectional FGM plate in ABAQUS using python code, the structural responses are studied. To check the correctness of our present model, a verification study is carried out for both the vibration and buckling behavior of the plate. After validation, the natural frequency and buckling characteristics of the composite plate are studied for unidirectionally and bidirectionally graded FGM plates with different grading patterns, and the effect of various parameters such as porosity and power-law indices, aspect ratio, thickness ratio etc. is studied.

Validation

The present method has been validated by relating the current results and available articles. Validation has been done for vibration and buckling conditions separately. For validating the vibrational and buckling responses, the current results are compared with the published values in [14] and [52], respectively.

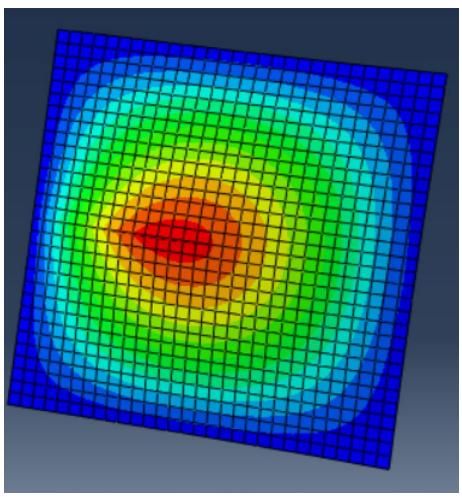

Fig. 8 First Mode of vibration in cracked FGM plate

Validation for Vibration Analysis

The validation of the present model for vibration study has been performed here by comparing the obtained results with the available data in [14] and presented in Table 1. The table shows that the obtained results matches the results in the published data is followed. The first three modes of vibration in ABAQUS are shown in Figs. 8, 9, 10. The natural frequency responses are presented in non-dimensional form for the validation purpose.

$$\Omega = \frac{\omega a^2}{h\sqrt{\frac{\rho_c}{E_c}}} \tag{7}$$

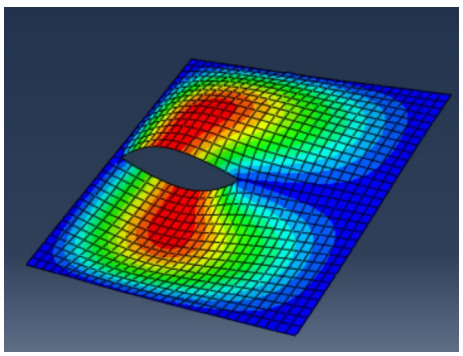

Fig. 9 Second mode of vibration in cracked FGM plate

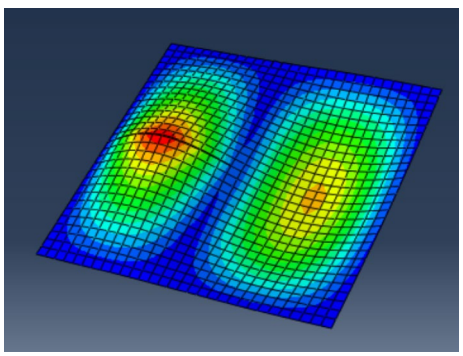

Fig. 10 Third mode of vibration in cracked FGM plate

where, ω is the natural frequency of the plate, ρ_c and E_c, respectively, are the mass density and Young's modulus of ceramic material. The materials used for validation are Aluminum (Al)/Alumina (Al_2O_3), having a square shape and thickness ratio of 10. The plate is SSSS at all the edges. The material properties for Al are $\nu_m = 0.3$, $\rho_m = 2702$ kg/m^3 and $E_m = 70$ GPa. Similarly, for Al_2O_3 $\nu_c = 0.3$, $\rho_c = 3800$ kg/m^3 and $E_c = 380$ GPa.

Validation for Buckling Analysis

The validation of the existing model for buckling analysis has been done by comparing the current results with the published responses [52] and presented in Table 2. The charted numbers indicated the accuracy of the present model as the error among the current and reference values lies within the acceptable range. The materials used are Al/Al_2O_3, having a square shape and thickness ratio of 10. The plate is SSSS at all the edges. The material properties for Al and Al_2O_3 are specified in the above subsection. The critical buckling load values are presented in non-dimensional form for the validation study.

$$\lambda_{cru} = \lambda_{crb} = \frac{Nb^2}{\pi^2 D} \tag{8}$$

where, λ_{cru} and λ_{crb} denote unidirectional and bidirectional critical buckling load, N denote externally applied in-plane mechanical load and D is expressed as:

$$D = \frac{E_c h^3}{12\left(1-\nu^2\right)} \tag{9}$$

Vibration Analysis

After the verification study, the parametric study for vibration and buckling analysis of FG plate structures is carried out. In the vibration analysis, Aluminum and Alumina are used as the FG materials. SSSS boundary condition is used for all the results, and the natural frequency is converted to non-dimensional form using the formula given in Eq. (7).

Table 3 Non-dimensional natural frequencies of cracked SSSS bidirectional FG plate ($a = b = 1$, $a/h = 10$, $n_x = 1$, $n_z = 5$)

FGM	Porosity index	Crack length (d)		
		0	0.25a	0.5a
P-FGM	0	3.7363	3.4263	3.2088
	0.1	2.8176	2.7942	2.6126
	0.2	1.6302	1.6150	1.5054
S-FGM	0	3.6057	3.5766	3.3476
	0.1	3.0156	2.9898	2.7949
	0.2	2.0445	2.0239	1.8865
E-FGM	0	4.6426	4.6157	4.3641
	0.1	4.2661	4.2413	4.0102
	0.2	3.9200	3.8973	3.6849

Effect of Crack Length and Porosity Index

The frequency responses of bidirectional FG plate are computed for a variety of crack lengths and porosity index and presented in Table 3. Tabulated data show that the values of the frequency declines as the rise in crack length. Also, as the porosity index upsurges, the natural frequency value declined for all the FG plates. With an introduction of crack or porosity, the stiffness of the plate declines, which leads to a decrease of frequency data.

Effect of Grading Indices (Unidirectional and Bi-Directional)

In Table 4, the impact of power exponents on the non-dimensional frequency of the cracked FG plate is shown. From table, it can be noted that as the grading index increases, the value of frequency decreases. This is due to the fact that as the grading index rises, the volume of metal in the FGM also rises, lowering the stiffness of the structure. Also, the comparison of unidirectional and bidirectional grading is shown here, which indicates that the frequency value decreases with the bidirectional grading as it impacts the stiffness more.

Table 2 Validation for buckling analysis of FGM plate

Reference	Critical buckling load (in MPa)					
	Power-law indices					
	$n_z = 0$		$n_z = 0.5$		$n_z = 1$	
	λ_{cru}	λ_{crb}	λ_{cru}	λ_{crb}	λ_{cru}	λ_{crb}
Ref. [52]	4.001	2.0002	2.7061	1.3531	2.2054	1.1028
Present	4.2302	2.0879	2.6945	1.3298	2.0939	1.0332
% difference	5.4182	4.2004	0.4305	1.7521	5.3249	6.7363

Table 4 Non-dimensional natural frequency of cracked SSSS uni/bidirectional FG plate ($a=b=1$, $a/h=10$, $d=0.5a$)

FGM	Porosity index	Unidirectional FGM ($n_x=0$)			Bidirectional FGM ($n_x=1$)		
		$n_z=0.5$	$n_z=2$	$n_z=5$	$n_z=0.5$	$n_z=2$	$n_z=5$
P-FGM	0	4.5621	3.7429	3.5224	3.7608	3.3354	3.2088
	0.1	4.3107	3.2448	2.9149	3.3480	2.7851	2.6126
	0.2	4.0167	2.4920	1.7473	2.7366	1.8719	1.5054
S-FGM	0	4.3027	3.9046	3.7075	3.6018	3.4313	3.3476
	0.1	4.0044	3.4789	3.2101	3.1566	2.9166	2.7949
	0.2	3.6433	2.8975	2.4857	2.4929	2.1019	1.8865
E-FGM	0	3.6832			4.3641		
	0.1	3.4428			4.0102		
	0.2	3.2181			3.6849		

Table 5 Non-dimensional natural frequency of cracked SSSS bidirectional FG plate ($a=1$, $a/h=10$, $d=0.5a$, $n_x=1$, $n_z=5$)

FGM	Porosity index	Aspect ratio (a/b)		
		2	1	0.5
P-FGM	0	6.3648	3.2088	2.1551
	0.1	5.1441	2.6126	1.7603
	0.2	2.9158	1.5054	1.0183
S-FGM	0	6.6756	3.3476	2.2427
	0.1	5.5353	2.7949	1.8742
	0.2	3.6360	1.8865	1.2678
E-FGM	0	9.0853	4.3641	2.8921
	0.1	8.3480	4.0102	2.6576
	0.2	7.6710	3.6849	2.4420

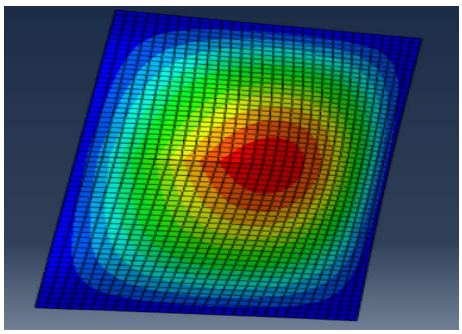

Fig. 11 Vibration in FGM plate with aspect ratio 0.5

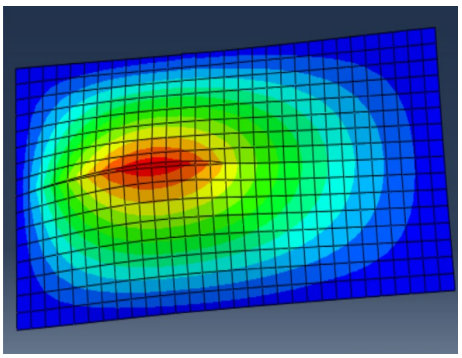

Fig. 12 Vibration in FGM plate with aspect ratio 2

Table 6 Non-dimensional critical buckling load of cracked SSSS bidirectional FG plate ($a=b=1$, $d=0.5a$, $n_x=1$, $n_z=5$)

FGM	Porosity index	Thickness ratio (a/h)		
		10	50	100
P-FGM	0	3.2088	3.3739	3.3855
	0.1	2.6126	2.7532	2.7632
	0.2	1.5054	1.5910	1.5970
S-FGM	0	3.3476	3.4942	3.5055
	0.1	2.7949	2.9158	2.9215
	0.2	1.8865	1.9675	1.9732
E-FGM	0	4.3641	4.5543	4.5681
	0.1	4.0102	4.1847	4.1976
	0.2	3.6849	3.8452	3.8572

Effect of Aspect Ratio

In Table 5, non-dimensional frequency of the bidirectional FG plate are provided for different aspect ratios. The relationship between the structure's length and stiffness is inverse. The structural stiffness reduces as length increases. Decreased stiffness leads to a fall in the frequency responses. The tabular data follow the same trend, i.e., frequency declines with an rise in aspect ratio (reduction in the width of the plate). Figures 11, 12 show the vibration in the FGM plate with an aspect ratio of 0.5 and 2, respectively.

Effect of Thickness Ratio

In Table 6, the variation of non-dimensional frequency responses for different values of thickness ratio is shown. The stiffness of the FG plate lowered down with an increase in thickness ratio (a/h) or decrease in thickness. Further,

the frequency responses of the bidirectional FG plate must decrease with an increase in thickness ratio (reduction of thickness). But tabulated data follows the reverse trend due to the non-dimensional form Eq. (7).

Buckling Analysis

After performing the frequency analysis, the model has been expanded to calculate the impact of various geometrical and material characteristics on the mechanical buckling strength,.To do so, a few numerical experimentations are carried out and discussed in the following lines. Aluminum and Alumina are used in the buckling analysis of FG materials. A UDL of magnitude 1 N/m^2 is applied, and the SSSS boundary condition is used to compute all the critical buckling load of the plate, which was then converted to non-dimensional form using Eq. (8).

Effect of Crack Length

The effect of crack length on the critical buckling load of the FG plate is presented in Table 7. With an upsurge in crack length, the stiffness of the FG plate decreases, which leads to a decrease in critical buckling load. But tabular data follow the reverse trend due to the non-dimensional form of the critical buckling load. Also, as the porosity index rises, the stiffness is decreased, and the critical buckling load also reduced for all the FG plates.

Effect of Grading Indices

The critical buckling load for the FG plate with respect to change in power exponents is computed and presented in Table 8. Due to a rise in the power-law exponent, the structure's stiffness decreases. Decreased stiffness leads to the decrease in the critical buckling load values of the FG plate, and tabulated data also show the same trend. The comparison of unidirectional and bidirectional grading is also shown in Table 8. Critical buckling load is less with bidirectional grading when compared to the unidirectional one.

Effect of Aspect Ratio

The critical buckling loads evaluated by changing the aspect ratio, grading type and porosity index values presented in

Table 7 Non-dimensional critical buckling load of cracked SSSS bidirectional FG plate ($a=b=1$, $a/h=10$, $n_x=1$, $n_z=5$)

FGM	Porosity index	Crack length (d)		
		0	0.25a	0.5a
P-FGM	0	1.3574	1.3619	1.5612
	0.1	0.9997	1.0021	1.1404
	0.2	0.6085	0.6075	0.6745
S-FGM	0	1.4993	1.5010	1.6494
	0.1	0.8977	1.1120	1.2123
	0.2	0.7143	0.7048	0.7489
E-FGM	0	3.3336	3.3458	3.8346
	0.1	3.0632	3.0895	3.5340
	0.2	2.8148	2.8251	3.1196

Table 9 Non-dimensional critical buckling load of cracked SSSS bidirectional FG plate ($a=1$, $a/h=10$, $d=0.5a$, $n_x=1$, $n_z=5$)

FGM	Porosity index	Aspect ratio (a/b)		
		2	1	0.5
P-FGM	0	0.2645	1.5612	7.0421
	0.1	0.1958	1.1404	5.1767
	0.2	0.1206	0.6745	3.1579
S-FGM	0	0.3055	1.6494	7.9550
	0.1	0.2331	1.2123	5.9571
	0.2	0.1552	0.7489	3.8224
E-FGM	0	0.6259	3.8346	17.2532
	0.1	0.5751	3.5340	15.8538
	0.2	0.5285	3.1196	14.5680

Table 8 Non-dimensional critical buckling load of cracked SSSS uni/bidirectional FG plate ($a=b=1$, $a/h=10$, $d=0.5a$)

FGM	Porosity index	Unidirectional FGM ($n_x=0$)			Bidirectional FGM ($n_x=1$)		
		$n_z=0.5$	$n_z=2$	$n_z=5$	$n_z=0.5$	$n_z=2$	$n_z=5$
P-FGM	0	3.2822	2.0362	1.7174	1.8790	1.4750	1.3619
	0.1	2.9492	1.6360	1.2935	1.5103	1.1067	1.0021
	0.2	2.6171	1.2044	0.8384	1.1111	0.7093	0.6075
S-FGM	0	2.7992	2.3283	2.1112	1.7223	1.5667	1.5010
	0.1	2.4627	1.9360	1.6942	1.3632	1.1925	1.1120
	0.2	2.1227	1.5246	1.2509	0.9766	0.7921	0.7048
E-FGM	0	2.1612			3.3458		
	0.1	1.9857			3.0745		
	0.2	1.8245			2.8251		

Table 10 Non-dimensional critical buckling load of cracked SSSS bidirectional FG plate ($a=b=1$, $d=0.5a$, $n_x=1$, $n_z=5$)

FGM	Porosity index	Thickness ratio (a/h)		
		10	50	100
P-FGM	0	1.5612	1.7056	1.7158
	0.1	1.1404	1.2427	1.2497
	0.2	0.6745	0.7313	0.7351
S-FGM	0	1.6494	1.7606	1.7682
	0.1	1.2123	1.2852	1.2906
	0.2	0.7489	0.7861	0.7887
E-FGM	0	3.8346	4.1419	4.1652
	0.1	3.5340	3.8060	3.8273
	0.2	3.1196	3.4973	3.5169

Table 9. With an increase in length, the stiffness of any structure decreases. The stiffness and buckling load are directly proportional to each other. Therefore, the buckling load should follow decreasing trend with an increase in aspect ratio, but tabular data depicts the reverse trend due to the non-dimensional form.

Effect of Thickness Ratio

In Table 10, the variation of critical buckling loads for various values of thickness ratio and porosity index is shown. With a rise in thickness ratio (a/h) or reduction in total thickness, the structural stiffness falls down, which leads to the reduction in critical buckling load. But critical buckling load in tabular data increases with an increase in thickness ratio due to the non-dimensional form expressed in Eq. (8). It can also observed from the tabular data that the increase in critical buckling load due to an increase in thickness ratio is far less than that due to increase in porosity index.

Conclusion

The python code has been utilized to develop a batch module to compute the eigenvalues (natural frequency responses and critical buckling load) of the bidirectional graded cracked porous structure. The model's efficacy has been proved by comparing the results with the data available from different domains. A few generalized understandings are obtained, i.e., the cracks cause a substantial decrement in total structural stiffness, which, in turn, reduces the final results adequately. Thin structural components are affected due to the presence of a crack in specific orientations, like in the lengthier edge of the rectangular shape. Also, it is possible to cause the propagation of the damage, which may further reduce the structural integrity and strength enormously.

Similarly, the porosity decreases the total stiffness and associated responses like the frequency and the critical buckling load parameters. The study indicates a minor influence of porosity for the exponential type of graded structure compared to all other grading patterns. Additionally, the final failures may affect factors like grading index and type of grading, as both cause an extreme change in the overall effective material properties. Finally, the study helps the designer choose the type of grading, porosity and other relevant parameters with damage for a suitable grading structure. The results show that the P-FGM will be the most flexible structural configuration compared to different types, including the damage and/or porosity.

Data availability There is no such third-party data has been utilized in this analysis. However, the generated data in the form of results are already within the text, and if anything more is required can be provided with a reasonable request.

Declarations

Conflict of interest The authors declare that they have no known competing financial interests or personal relationships that could have appeared to influence the work reported in this paper.

References

1. Stahl B, Keer LM (1972) Vibration and stability of cracked rectangular plates. Int J Solids Struct 8:69–91. https://doi.org/10.1016/0020-7683(72)90052-2
2. Kumar YVS, Paik JK (2004) Buckling analysis of cracked plates using hierarchical trigonometric functions. Thin-Walled Struct 42:687–700. https://doi.org/10.1016/j.tws.2003.12.012
3. Brighenti R (2005) Numerical buckling analysis of compressed or tensioned cracked thin plates. Eng Struct 27:265–276. https://doi.org/10.1016/j.engstruct.2004.10.006
4. Devarajan B, Kapania RK (2022) Analyzing thermal buckling in curvilinearly stiffened composite plates with arbitrary shaped cutouts using isogeometric level set method. Aerosp Sci Technol. https://doi.org/10.1016/j.ast.2022.107350
5. Devarajan B, Kapania RK (2020) Thermal buckling of curvilinearly stiffened laminated composite plates with cutouts using isogeometric analysis. Compos Struct 238:111881. https://doi.org/10.1016/j.compstruct.2020.111881
6. Miglani J, Devarajan B, Kapania RK (2018) Thermal buckling analysis of periodically supported laminated beams using isogeometric analysis. AIAA/ASCE/AHS/ASC Struct, Struct Dyn Mater Conf. https://doi.org/10.2514/6.2018-1224
7. Fan F, Cai X, Sahmani S, Safaei B (2021) Isogeometric thermal postbuckling analysis of porous FGM quasi-3D nanoplates having cutouts with different shapes based upon surface stress elasticity. Compos Struct 262:113604. https://doi.org/10.1016/j.compstruct.2021.113604
8. Ghanati P, Safaei B (2019) Elastic buckling analysis of polygonal thin sheets under compression. Indian J Phys 93:47–52. https://doi.org/10.1007/s12648-018-1254-9

9. Yang J, Chen Y (2008) Free vibration and buckling analyses of functionally graded beams with edge cracks. Compos Struct 83:48–60. https://doi.org/10.1016/j.compstruct.2007.03.006
10. Fattahi AM, Safaei B (2017) Buckling analysis of CNT-reinforced beams with arbitrary boundary conditions. Microsyst Technol 23:5079–5091. https://doi.org/10.1007/s00542-017-3345-5
11. Talha M, Singh BN (2011) Thermo-mechanical buckling analysis of finite element modeled functionally graded ceramic-metal plates. Int J Appl Mech 3:867–880. https://doi.org/10.1142/S1758825111001275
12. Cheshmeh E, Karbon M, Eyvazian A et al (2022) Buckling and vibration analysis of FG-CNTRC plate subjected to thermo-mechanical load based on higher order shear deformation theory. Mech Based Des Struct Mach 50:1137–1160. https://doi.org/10.1080/15397734.2020.1744005
13. Huang CS, McGee IG, Chang MJ (2011) Vibrations of cracked rectangular FGM thick plates. Compos Struct 93:1747–1764. https://doi.org/10.1016/j.compstruct.2011.01.005
14. Natarajan S, Baiz PM, Bordas S et al (2011) Natural frequencies of cracked functionally graded material plates by the extended finite element method. Compos Struct 93:3082–3092. https://doi.org/10.1016/j.compstruct.2011.04.007
15. Amiri Rad A, Panahandeh-Shahraki D (2014) Buckling of cracked functionally graded plates under tension. Thin-Walled Structures 84:26–33. https://doi.org/10.1016/j.tws.2014.05.005
16. Tran LV, Ly HA, Lee J et al (2015) Vibration analysis of cracked FGM plates using higher-order shear deformation theory and extended isogeometric approach. Int J Mech Sci 96–97:65–78. https://doi.org/10.1016/j.ijmecsci.2015.03.003
17. Kandasamy R, Dimitri R, Tornabene F (2016) Numerical study on the free vibration and thermal buckling behavior of moderately thick functionally graded structures in thermal environments. Compos Struct 157:207–221. https://doi.org/10.1016/j.compstruct.2016.08.037
18. Nuhu AA, Safaei B (2022) State-of-the-art of vibration analysis of small-sized structures by using nonclassical continuum theories of elasticity. Springer, Netherlands
19. Yi H, Sahmani S, Safaei B (2020) On size-dependent large-amplitude free oscillations of FGPM nanoshells incorporating vibrational mode interactions. Arch Civil Mech Eng. https://doi.org/10.1007/s43452-020-00047-9
20. Safaei B (2021) Frequency-dependent damped vibrations of multifunctional foam plates sandwiched and integrated by composite faces. Eur Phys J Plus 136:646. https://doi.org/10.1140/epjp/s13360-021-01632-4
21. Yang X, Sahmani S, Safaei B (2021) Postbuckling analysis of hydrostatic pressurized FGM microsized shells including strain gradient and stress-driven nonlocal effects. Eng with Computers 37:1549–1564. https://doi.org/10.1007/s00366-019-00901-2
22. Abdussalam A, Safaei B (2022) Thin-walled structures a comprehensive review on the vibration analyses of small-scaled plate-based structures by utilizing the nonclassical continuum elasticity theories. Thin-Walled Struct 179:109622. https://doi.org/10.1016/j.tws.2022.109622
23. Hadji L, Avcar M, Zouatnia N (2022) Natural frequency analysis of imperfect FG sandwich plates resting on Winkler-Pasternak foundation. Mater Today: Proceed 53:153–160. https://doi.org/10.1016/j.matpr.2021.12.485
24. Hadji L, Avcar M (2021) Free vibration analysis of FG porous sandwich plates under various boundary conditions. J Appl Computational Mech 7:505–519. https://doi.org/10.22055/jacm.2020.35328.2628
25. Avcar M (2019) Free vibration of imperfect sigmoid and power law functionally graded beams. Steel Compos Struct, Int J 30(6):603–615. https://doi.org/10.12989/scs.2019.30.6.603
26. Hadji L, Avcar M (2021) Nonlocal free vibration analysis of porous FG nanobeams using hyperbolic shear deformation beam theory. Adv Nano Res 10:281–293. https://doi.org/10.12989/ANR.2021.10.3.281
27. Nasirmanesh A, Mohammadi S (2015) XFEM buckling analysis of cracked composite plates. Compos Struct 131:333–343. https://doi.org/10.1016/j.compstruct.2015.05.013
28. Liu P, Bui TQ, Zhu D et al (2015) Buckling failure analysis of cracked functionally graded plates by a stabilized discrete shear gap extended 3-node triangular plate element. Compos B Eng 77:179–193. https://doi.org/10.1016/j.compositesb.2015.03.036
29. Demir Ç, Mercan K, Civalek O (2016) Determination of critical buckling loads of isotropic, FGM and laminated truncated conical panel. Compos B Eng 94:1–10. https://doi.org/10.1016/j.compositesb.2016.03.031
30. Nasirmanesh A, Mohammadi S (2017) An extended finite element framework for vibration analysis of cracked FGM shells. Compos Struct 180:298–315. https://doi.org/10.1016/j.compstruct.2017.08.019
31. Gupta A, Jain NK, Salhotra R (2017) Effect of crack orientation on vibration characteristics of partially cracked FGM plate: an analytical approach. Mater Today: Proceed 4:10179–10183. https://doi.org/10.1016/j.matpr.2017.06.344
32. Milazzo A, Benedetti I, Gulizzi V (2018) An extended Ritz formulation for buckling and post-buckling analysis of cracked multilayered plates. Compos Struct 201:980–994. https://doi.org/10.1016/j.compstruct.2018.06.026
33. Yin BB, Lei Z (2022) Vibration characteristics of cracked FG-GRC plates in thermal environments based on phase field theory and meshless method. Mech Based Des Struct Mach. https://doi.org/10.1080/15397734.2022.2047722
34. Singh SK, Singh IV, Mishra BK et al (2018) Analysis of cracked plate using higher-order shear deformation theory: asymptotic crack-tip fields and XIGA implementation. Comput Methods Appl Mech Eng 336:594–639. https://doi.org/10.1016/j.cma.2018.03.009
35. Milazzo A, Benedetti I, Gulizzi V (2019) A single-domain Ritz approach for buckling and post-buckling analysis of cracked plates. Int J Solids Struct 159:221–231. https://doi.org/10.1016/j.ijsolstr.2018.10.002
36. Ramteke PM, Patel B, Panda SK (2020) Time-dependent deflection responses of porous FGM structure including pattern and porosity. Int J Appl Mech 12:1–26. https://doi.org/10.1142/S1758825120501021
37. Karamanli A, Aydogdu M (2020) Bifurcation buckling conditions of FGM plates with different boundaries. Compos Struct 245:112325. https://doi.org/10.1016/j.compstruct.2020.112325
38. Ghayesh MH, Amabili M (2013) Post-buckling bifurcations and stability of high-speed axially moving beams. Int J Mech Sci 68:76–91. https://doi.org/10.1016/j.ijmecsci.2013.01.001
39. Zhu LF, Ke LL, Xiang Y, Zhu XQ (2020) Free vibration and damage identification of cracked functionally graded plates. Compos Struct 250:112517. https://doi.org/10.1016/j.compstruct.2020.112517
40. Al Rjoub YS, Alshatnawi JA (2020) Free vibration of functionally-graded porous cracked plates. Structures 28:2392–2403. https://doi.org/10.1016/j.istruc.2020.10.059
41. Ramteke PM, Panda SK (2021) Free vibrational behaviour of multi-directional porous functionally graded structures. Arab J Sci Eng 46:7741–7756. https://doi.org/10.1007/s13369-021-05461-6
42. Ramteke PM, Sharma N, Choudhary J et al (2021) Multidirectional grading influence on static/dynamic deflection and stress responses of porous FG panel structure: a micromechanical approach. Eng with Computers. https://doi.org/10.1007/s00366-021-01449-w

43. Sitli Y, Mhada K, Bourihane O, Rhanim H (2021) Buckling and post-buckling analysis of a functionally graded material (FGM) plate by the asymptotic numerical method. Structures 31:1031–1040. https://doi.org/10.1016/j.istruc.2021.01.100
44. Hu Z, Zheng X, An D et al (2021) New analytic buckling solutions of side-cracked rectangular thin plates by the symplectic superposition method. Int J Mech Sci 191:106051. https://doi.org/10.1016/j.ijmecsci.2020.106051
45. Khatir S, Tiachacht S, Le Thanh C et al (2021) An improved artificial neural network using arithmetic optimization algorithm for damage assessment in FGM composite plates. Compos Struct 273:114287. https://doi.org/10.1016/j.compstruct.2021.114287
46. Kumar Sah S, Ghosh A (2022) Influence of porosity distribution on free vibration and buckling analysis of multi-directional functionally graded sandwich plates. Compos Struct 279:114795. https://doi.org/10.1016/j.compstruct.2021.114795
47. Kolahchi R (2017) A comparative study on the bending, vibration and buckling of viscoelastic sandwich nano-plates based on different nonlocal theories using DC, HDQ and DQ methods. Aerosp Sci Technol 66:235–248. https://doi.org/10.1016/J.AST.2017.03.016
48. Sinha GP, Kumar B (2021) Review on vibration analysis of functionally graded material structural components with cracks. J Vib Eng Technol 9:23–49. https://doi.org/10.1007/s42417-020-00208-3
49. Ramteke PM, Panda SK, Patel B (2022) Nonlinear eigenfrequency characteristics of multi-directional functionally graded porous panels. Compos Struct 279:114707. https://doi.org/10.1016/j.compstruct.2021.114707
50. Chi S-H, Chung Y-L (2006) Mechanical behavior of functionally graded material plates under transverse load—part I: analysis. Int J Solids Struct 43:3657–3674. https://doi.org/10.1016/j.ijsolstr.2005.04.011
51. Ramteke PM, Panda SK, Sharma N (2022) Nonlinear vibration analysis of multidirectional porous functionally graded panel under thermal environment. AIAA J. https://doi.org/10.2514/1.J061635
52. Ganapathi M, Prakash T, Sundararajan N (2006) Influence of functionally graded material on buckling of skew plates under mechanical loads. J Eng Mech 132:902–905. https://doi.org/10.1061/(ASCE)0733-9399(2006)132:8(902)